A comparative Assessment of Moment-Based Closures for Flows at Various Levels of Rarefaction

P. Bernigaud[1], D. Biasone[1,2], S. Dubois[2], A. Hoffmann[2], M. Massot[2]

[1]DMPE, ONERA, Université Paris-Saclay
[2]CMAP, CNRS, École polytechnique

CANUM 2026

Overview

Table of contents

Context and Motivation

Hybrid dense–rarefied flow fields

- Strong spatial variations of *Knudsen* number
- Coexistence of multiple regimes
- Portions of domain under transition regime conditions

Examples of applications

- **Rocket propulsion plumes**
  (dense core → rarefied far field)
- **Atmospheric re-entry / planetary descent**
  (dense shock → rarefied wake)
- **High-altitude hypersonic flight**
  (boundary layer → rarefied exterior)

Saturn V exhaust plume during the launch of Apollo 11

Context and Motivation

Hybrid dense–rarefied flow fields

- Strong spatial variations of *Knudsen* number
- Coexistence of multiple regimes
- Portions of domain under transition regime conditions

Examples of applications

- **Rocket propulsion plumes**
  (dense core → rarefied far field)
- **Atmospheric re-entry / planetary descent**
  (dense shock → rarefied wake)
- **High-altitude hypersonic flight**
  (boundary layer → rarefied exterior)

SpaceX Starship hypersonic flight

Context and Motivation

Hybrid dense–rarefied flow fields

- Strong spatial variations of *Knudsen* number
- Coexistence of multiple regimes
- Portions of domain under transition regime conditions

Examples of applications

- **Rocket propulsion plumes**
  (dense core → rarefied far field)
- **Atmospheric re-entry / planetary descent**
  (dense shock → rarefied wake)
- **High-altitude hypersonic flight**
  (boundary layer → rarefied exterior)

Mockup of ESA shuttle Hermes

Rarefaction and Knudsen number

Knudsen number

$$\mathrm{Kn} = \frac{\lambda}{\ell}$$

ratio between mean free path λ and a characteristic length ℓ Cercignani, (1990)

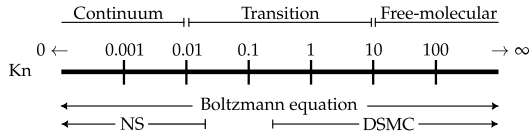

Numerical methods (Torrilhon, (2016))

- $\mathrm{Kn} \ll 1$: **continuum regime** → well described by Euler/NS (CFD)
- $\mathrm{Kn} \gg 1$: **free molecular regime** → requires kinetic description (Boltzmann, DSMC)
- $10^{-2} < \mathrm{Kn} < 10^{1}$: **transition regime** → no universally accepted best practice

State-of-the-art of modelling frameworks for rarefied flows

Classical approaches

Kinetic solvers (Boltzmann, DSMC)

- Accurate for rarefied regimes
- *Prohibitively expensive* as $\mathrm{Kn} \to 0$[(1)]

Continuum solvers (CFD / NS)

- Efficient in dense regions
- *Break down* in non-equilibrium regimes[(2)]

Hybrid NS/DSMC methods[(3)]

- Combine efficiency and accuracy across regimes
- *Interface definition is non-trivial*[(4)], domain decomposition challenges
- Coupling strategy not straightforward

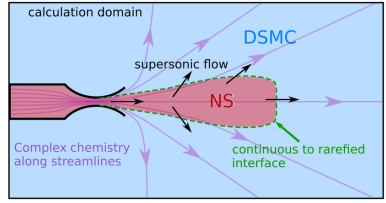

Domain partition in hybrid NS–DSMC (Virgile et al., (2022))

⇒ **Reliable prediction of transition-regime flows remains challenging**

(1) Yang et al., (2019) (2) Ferziger et al., (1973) (3) Schwartzentruber et al., (2006) (4) Xu et al., (2010)

Method of Moments: a reduced kinetic approach

Underlying principles

- Macroscopic quantities are *moments* of the distribution function
- Many applications require only a *limited subset* of these moments
- Evolve moment equations instead of full VDF

Key advantages

- Provides a *reduced kinetic description*[(1)]
- More accurate than NS: captures *non-equilibrium effects*
- Much *cheaper* than full kinetic solver

Current challenges

- Mathematical structure, boundary conditions, etc.
- Presence of *sub-shocks* in some formulations
- *Multiple closure models* available
- **Uncertainty: which closure is the *most effective*?**

Contribution of this work: Systematic benchmark and evaluation of existing closure methodologies for the method of moments in resolving transitional rarefied flow fields

(1) Torrilhon, (2010)

Table of contents

Kinetic description of a gas

Core idea

- Instead of tracking $\sim 10^{23}$ particles, describe the gas via a *distribution function* $f(t, x, v)$
- $f \, \mathrm{d}x \, \mathrm{d}v =$ number of particles near position x with velocity v at time t
- **1D1V setting:** $x \in \mathbb{R}, \quad v \in \mathbb{R}$

Governing equation

The evolution of f is governed by the **Boltzmann equation** (Cercignani et al., (1994); Villani, (2002))

$$\underbrace{\frac{\partial f}{\partial t} + v \frac{\partial f}{\partial x}}_{\text{free streaming}} = \underbrace{\mathcal{Q}(f, f)}_{\text{collisions}}$$

Kinetic description of a gas

Core idea

- Instead of tracking $\sim 10^{23}$ particles, describe the gas via a *distribution function* $f(t,x,v)$
- $f\,\mathrm{d}x\,\mathrm{d}v$ = number of particles near position x with velocity v at time t
- **1D1V setting:** $x \in \mathbb{R},\ \ v \in \mathbb{R}$

Governing equation

The evolution of f is governed by the **Boltzmann equation** (Cercignani et al., (1994); Villani, (2002))

$$\underbrace{\frac{\partial f}{\partial t} + v\frac{\partial f}{\partial x}}_{\text{free streaming}} = \underbrace{\mathcal{Q}(f,f)}_{\text{collisions}}$$

Collision operator $\mathcal{Q}(f,f)$

Models the effect of binary collisions:

- BGK (relaxation model)
- Hard spheres
- ES–BGK, Fokker–Planck, ...

Kinetic description of a gas

Core idea

- Instead of tracking $\sim 10^{23}$ particles, describe the gas via a *distribution function* $f(t, x, v)$
- $f \, \mathrm{d}x \, \mathrm{d}v =$ number of particles near position x with velocity v at time t
- **1D1V setting:** $x \in \mathbb{R}, \quad v \in \mathbb{R}$

Governing equation

The evolution of f is governed by the **Boltzmann equation** (Cercignani et al., (1994); Villani, (2002))

$$\underbrace{\frac{\partial f}{\partial t} + v \frac{\partial f}{\partial x}}_{\text{free streaming}} = \underbrace{\mathcal{Q}(f, f)}_{\text{collisions}}$$

BGK modelling: Relaxation toward equilibrium

- Collisions drive f toward a **local Maxwellian** $\mathcal{M}$ (Bhatnagar et al., (1954))
- $\tau \propto \mathrm{Kn}$: relaxation time

$$\mathcal{Q}_{\mathrm{BGK}}(f, f) = \frac{1}{\tau}(\mathcal{M} - f)$$

$$\mathcal{M}(v) = \frac{\rho}{\sqrt{2\pi\theta}} \exp\left[-\frac{(v-u)^2}{2\theta}\right]$$

From kinetic to macroscopic: velocity moments

Key observation: all macroscopic quantities are *velocity moments* of f (Groth, (2020))

Convective moments

$$M_k = m \int_{\mathbb{R}} v^k f \, \mathrm{d}v$$

$M_0 = \rho$ (density)

$M_1 = \rho u$ (momentum)

$M_2 = \rho u^2 + 2\rho e$ (energy)

$\dots$

Central moments

$$C_k = m \int_{\mathbb{R}} (v-u)^k f \, \mathrm{d}v$$

$C_0 = 1, \quad C_1 = 0$

$C_2 = p$ (pressure)

$C_3 = 2q$ (heat flux)

$\dots$

Method of moments: derive conservation equations for a finite set of moments $\rightarrow$ kinetic equation simplified into fluid model

Moment equations: from kinetic to fluid-like

Start from the Boltzmann equation and apply the *moment operator*:

$$\langle \cdot \rangle_k := m \int_{\mathbb{R}} v^k \, (\cdot) \, \mathrm{d}v$$

$$\frac{\partial}{\partial t} \underbrace{\left(m \int_{\mathbb{R}} v^k f \, \mathrm{d}v \right)}_{M_k} + \frac{\partial}{\partial x} \underbrace{\left(m \int_{\mathbb{R}} v^{k+1} f \, \mathrm{d}v \right)}_{M_{k+1}} = \langle m \, v^k \, \mathcal{Q} \rangle$$

Repeated for $k = 0, \ldots, n-1$ yields the **moment system**:

$$\frac{\partial M_k}{\partial t} + \frac{\partial M_{k+1}}{\partial x} = \langle m \, v^k \, \mathcal{Q}(f, f) \rangle$$

Key features

- Finite set of macroscopic conservation laws
- Retains non-equilibrium physics beyond standard NS
- Higher-order moments (stress, heat flux) become *independent state variables*

Recovered models by truncation order

$n = 3$	Euler equations (density, momentum, energy)
$n = 5$	Extended NS equations (+ stress tensor, heat flux as independent variables)
$n \to \infty$	Full kinetic description

The closure problem

Where does the problem arise?

Retaining $(M_0, \dots, M_{n-1})$ and writing the equation for the last moment M_{n-1}:

$$\frac{\partial M_{n-1}}{\partial t} + \frac{\partial M_n}{\partial x} = \langle m\, v^{n-1}\, \mathcal{Q} \rangle$$

The flux M_n is **not** in our set of unknowns: the system is *underdetermined*.

Closure problem

To close the system, one must express M_n in terms of the retained moments $(M_0, \dots, M_{n-1})$

Closure strategy

Introduce an *approximate* distribution $\hat{f}$, reconstructed from the retained moments:

$$f \approx \hat{f} = \mathcal{F}(M_0, \dots, M_{n-1})$$
$$M_n \approx \hat{M}_n = m \int_{\mathbb{R}} v^n \hat{f}\, \mathrm{d}v$$

What defines a good closure?

- Consistent with known equilibrium limits
- Hyperbolic system (finite wave speeds)
- Entropy inequality satisfied

The choice of $\mathcal{F}$ is the central question of the moment method $\rightarrow$ many strategies exist

Table of contents

Closure strategies: overview

Truncating the moment hierarchy requires a *closure* for the highest-order moment

A well-posed closure should satisfy (Laurent et al., (2024); Pichard, (2023)):

- **a.** **Realizability**: moments correspond to a non-negative distribution
- **b.** **Existence**: closure defined for all realizable states
- **c.** **Hyperbolicity**: well-posed PDE system
- **d.** **Thermodynamic consistency**: correct equilibria and entropy dissipation
- ⋆ **Efficiency**: low computational cost

Numerous closures have been proposed in the literature, with a strong impact on both *accuracy* and *mathematical structure* of the resulting system

Closure strategies: the three families

Grad-type

Expansion around a Maxwellian via Hermite polynomials

Classical Grad Grad, (1949)

Accurate near equilibrium, not globally hyperbolic

Linearized Grad Hu et al., (2020)

Spectral formulation, globally hyperbolic

Quadrature-based

VDF approximated as weighted sum of kernels

Bi-Gaussian Chalons et al., (2017)

Gaussian kernels, smooth reconstruction

HyQMOM Fox et al., (2018)

Dirac kernels, Chebyshev-based inversion

Entropy-based

Ansatz from entropy optimisation problem

MaxEnt Levermore, (1996)

Exponential distribution ansatz

Phi-divergence Abdelmalik et al., (2016)

Deformed exponential, truncated power approximation

Closure strategies: trade-offs

Closure	Hyperbolicity	Realizability	Cost	Multi-D
Classical Grad	weak	✓	medium	easy
Linearized Grad	✓	✓	medium	easy
Bi-Gaussian	✓	partial	large	difficult
HyQMOM	✓	✓	low	difficult
MaxEnt	✓	partial	large	limited
Phi-divergence	✓	✓	large	limited

No universally optimal closure: trade-offs between accuracy, robustness, and computational cost motivate a systematic benchmark

Table of contents

Methodology: assessment strategy

Gap in literature: Limited systematic comparison of closure methods in transitional regime

Goal: Quantitative comparison of closure performance across representative test cases

Benchmark setup

- 1D stationary shock structures
- Riemann problem with Rankine–Hugoniot initial states
- Monatomic argon gas

Test matrix

- Mach numbers: $\mathrm{Ma} = 2,\ 4$
- Knudsen numbers: $\mathrm{Kn} = 0.1,\ 1.0$

Reference solution

- Discrete Velocity Method (DVM)
- Phase space discretization

$$[x_L, x_R] \times [v_L, v_R] \qquad N_x = 10^4,\ N_v = 400$$

with velocity range $v \in [-10, 10]$

Methodology: moment-model solver

5-Moment system

$$\frac{\partial \mathbf{M}(\mathbf{Q})}{\partial t} + \frac{\partial \mathbf{F}(\mathbf{Q})}{\partial x} = \mathbf{S}(\mathbf{Q}), \qquad \mathbf{M} = (M_0, \dots, M_4)^\mathsf{T}$$

$\mathbf{Q} = (\rho, u, p, q, r)^\mathsf{T}$ primitive variables

$\mathbf{F}(\mathbf{Q})$ depends on the chosen closure

Implementation

- SAMURAI[(1)] framework (meshing, ghost cells, parallelization)
- Uniform 1D grid: 16384 cells
- First-order scheme to isolate intrinsic closure capabilities

Numerical strategy: operator splitting

1. Advection step
HLL approximate Riemann solver
explicit Euler time integration

↓

2. Collision step
BGK operator
exact analytical integration

↓

Repeated each time step
until steady state

(1) github.com/hpc-maths/samurai

Test case: 1D shock structure

Initial condition

Discontinuity at $x = 0$ between two Maxwellian states:

$$f(0,x,v) = \begin{cases} \mathcal{M}_L(v), & x < 0 \\ \mathcal{M}_R(v), & x > 0 \end{cases}$$

Macroscopic states from Rankine–Hugoniot:

$$(\rho_L, u_L, \theta_L) = \left(1,\ \sqrt{3}\,\mathrm{Ma},\ 1\right)$$

$$(\rho_R, u_R, \theta_R) = \left(\frac{2\mathrm{Ma}^2}{\mathrm{Ma}^2+1},\ \frac{\sqrt{3}}{2}\,\frac{\mathrm{Ma}^2+1}{\mathrm{Ma}},\ \frac{(3\mathrm{Ma}^2-1)(\mathrm{Ma}^2+1)}{4\mathrm{Ma}^2}\right)$$

Free parameters: Ma and Kn

Density profile $\rho(x)$ at $t = 0$

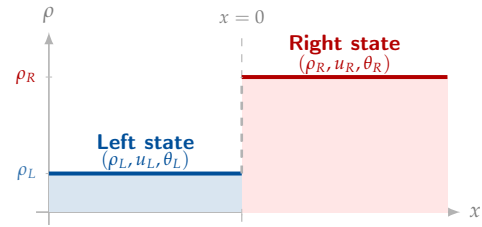

The system evolves toward a *steady shock structure* ⇒ comparison against the DVM reference

Table of contents

Solution in non-dimensional moment space

Normalised moments

$$q^* = \frac{q}{p^{3/2}}, \qquad r^* = \frac{r}{p^2}$$

Equilibrium fixed point

$$(q^*, r^*) = (0, 3)$$

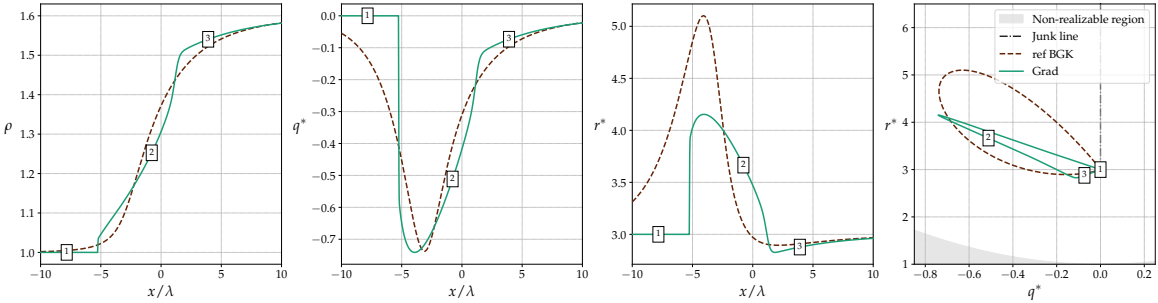

Trajectory in (q^*, r^*) space through the shock structure — Grad closure vs. BGK reference, $\mathrm{Kn} = 0.1$, $\mathrm{Ma} = 2$

Comparison at Ma = 2 – density

Sub-shocks

- **Grad, HyQMOM:** intrinsic property of ansatz
- **MaxEnt:** finite integration domain

Smooth profiles

- **Lin. Grad, Bi-Gaussian, φ-div**: evolution closer to reference

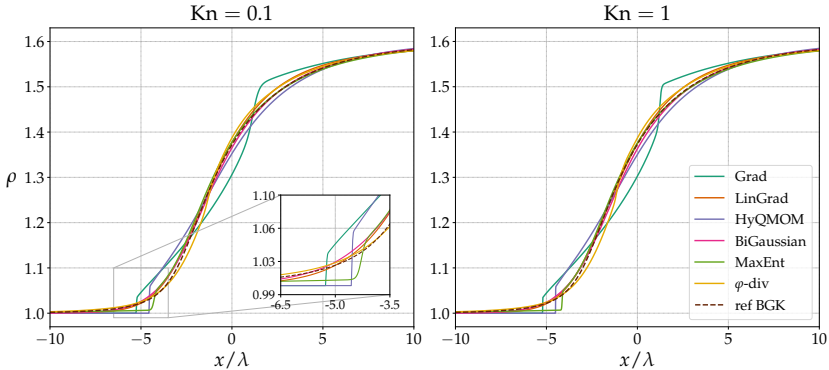

Non dimensional density profiles for two test cases. Spatial coordinate scaled with respect to mean free path

Comparison at Ma = 2 – heat flux

Sub-shocks

- **Grad, HyQMOM:** intrinsic property of ansatz
- **MaxEnt:** finite integration domain

Smooth profiles

- **Lin. Grad, Bi-Gaussian, φ-div**: evolution closer to reference

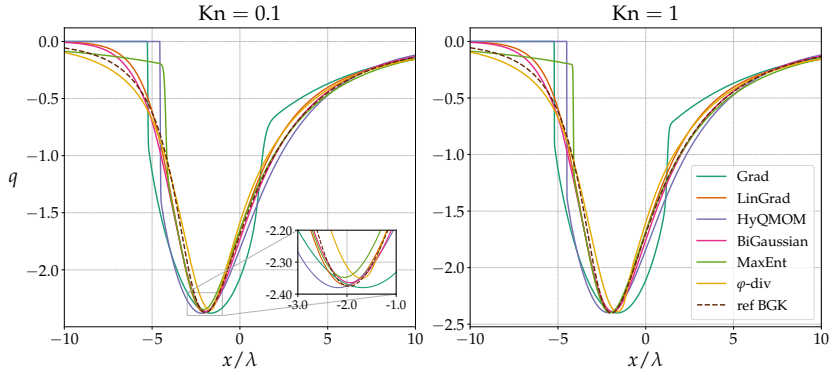

Non dimensional heat flux profiles for two test cases. Spatial coordinate scaled with respect to mean free path

Comparison at Ma = 2 – non-dimensional moment space

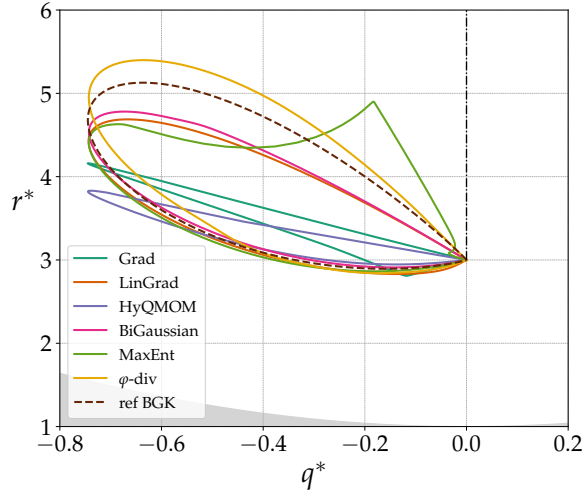

Comparison of moment solutions in normalized moment space, $\mathrm{Kn} = 1, \mathrm{Ma} = 2$

Comparison at Ma = 4 – density

Failures
- **Grad:** loss of hyperbolicity
- **MaxEnt:** optimisation diverges

Larger deviations
- **HyQMOM:** strong sub-shock
- **LinGrad, φ-div:** deviation at shock front, due to sensitivity to modelling parameters

Most accurate
- **Bi-Gaussian:** closer to reference

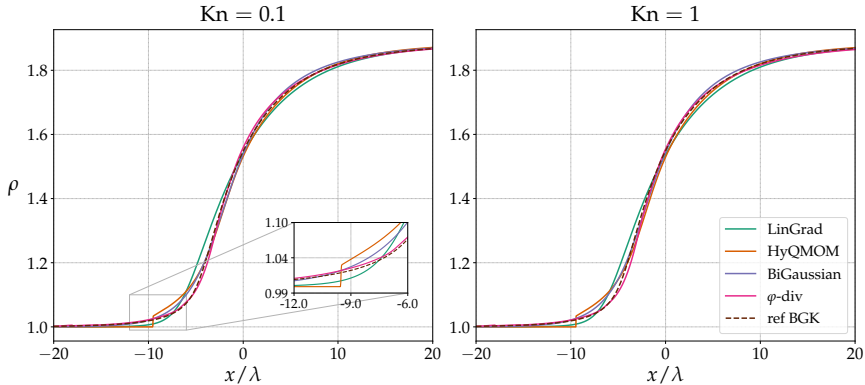

Non dimensional density profiles for two test cases. Spatial coordinate scaled with respect to mean free path

Comparison at Ma = 4 – heat flux

Failures
- **Grad:** loss of hyperbolicity
- **MaxEnt:** optimisation diverges

Larger deviations
- **HyQMOM:** strong sub-shock
- **LinGrad, φ-div:** deviation at shock front, due to sensitivity to modelling parameters

Most accurate
- **Bi-Gaussian:** closer to reference

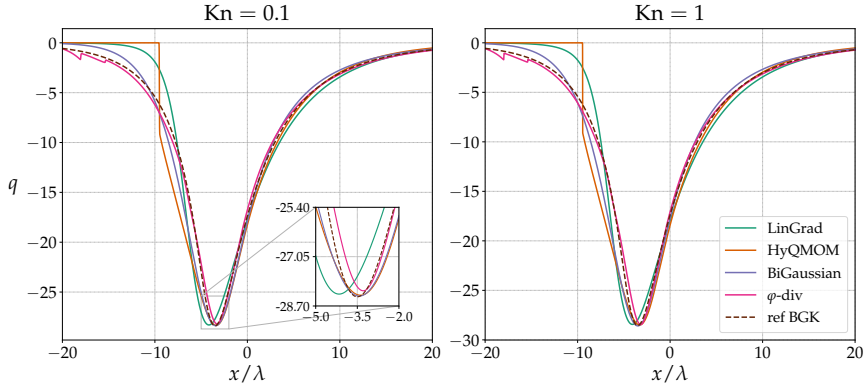

Non dimensional heat flux profiles for two test cases. Spatial coordinate scaled with respect to mean free path

Comparison at Ma = 4 – non-dimensional moment space

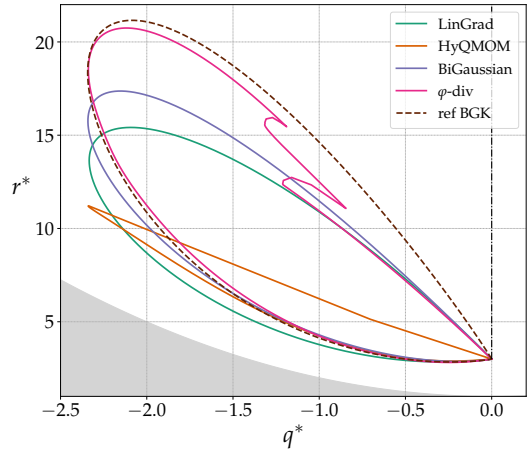

Comparison of moment solutions in normalized moment space, $\mathrm{Kn} = 1, \mathrm{Ma} = 4$

Computational efficiency

Cost of evaluating the closing moment

Method	Time [μs/cell]	vs. Grad	Inversion
HyQMOM	0.039	$\times 0.05$	direct
Grad	0.80	$\times 1.0$	direct
Linearized Grad	0.80	$\times 1.0$	direct
Bi-Gaussian	10.7	$\times 13$	iterative
Phi-divergence	16.5	$\times 21$	iterative
MaxEnt	24.0	$\times 30$	iterative

Times measured per cell evaluation, sorted by cost

Key takeaways

Fastest: HyQMOM

$20\times$ cheaper than Grad thanks to direct polynomial inversion, no iterative solve required

Grad / Lin. Grad

Essentially identical cost, polynomial evaluation only

Slowest: MaxEnt

$> 30\times$ Grad due to iterative optimisation at every cell and time step

Table of contents

Conclusions and perspectives

What this work established

Benchmark of six closure strategies across Mach and Knudsen numbers, with DVM reference

Key findings

- **Linearized Grad**: best overall compromise: accurate, robust, low cost, no realizability issues
- **HyQMOM**: fastest closure by far; sub-shocks remain without kinetic enrichment
- **Bi-Gaussian**: highest accuracy when applicable, limited by realizability domain
- **Entropy-based** closures: thermodynamically consistent but prohibitively costly

Ongoing and future work

- Testing of additional test cases to further assess the capabilities of the closures
- Analysis at larger number of moments
- Extension to *2D* problems [(1)]
- Participation to the 34th International Symposium on Rarefied Gas Dynamics (RGD34)

[(1)] Bernigaud et al., (2026)

Moment convergence

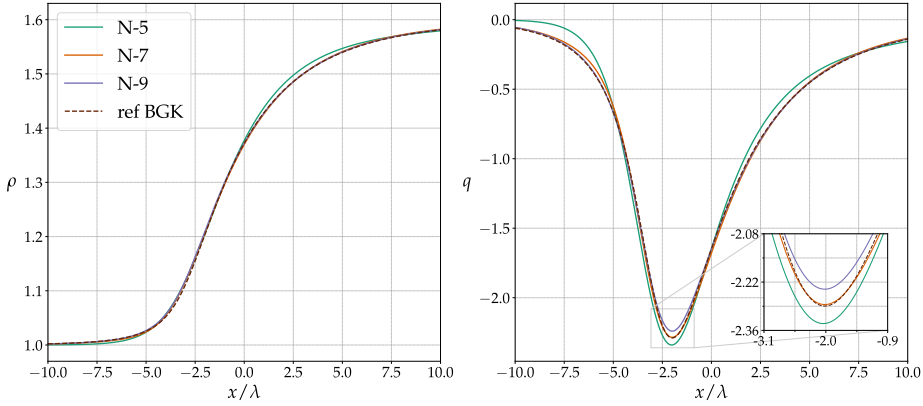

Moment solutions at increasing number of retained moments for Linearized Grad closure. Test case at $\mathrm{Ma} = 2$, $\mathrm{Kn} = 0.1$

Moment convergence (cont.)

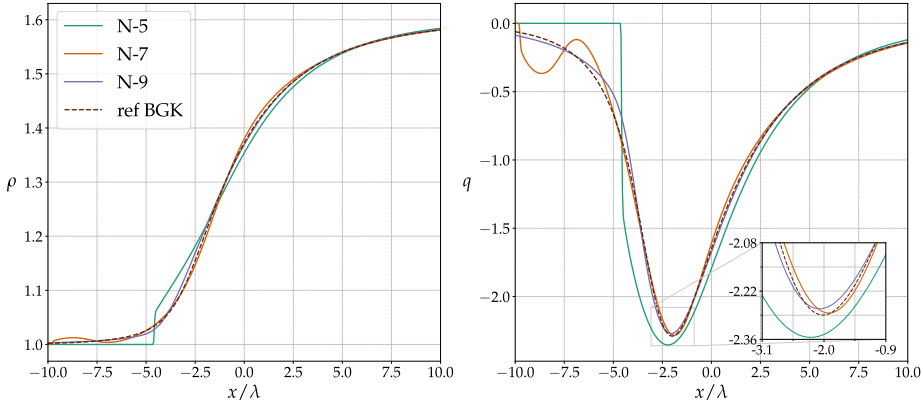

Moment solutions at increasing number of retained moments for HyQMOM closure. Test case at $\mathrm{Ma} = 2$, $\mathrm{Kn} = 0.1$

2D test case: expansion of rocket plume

Test case description

- Interaction of two co-flowing streams with different densities
- Idealized configuration representative of a rocket plume expansion at high altitude

- Inflow velocity: $u_0 = 300\,\mathrm{m/s}$
- Inflow temperature: $T_0 = 45\,\mathrm{K}$
- High-density stream: $\rho_+ = 3.5 \times 10^{-3}\,\mathrm{kg/m^3}$
- Low-density stream: $\rho_- = \rho_+/10$

Numerical setup and reference

- Moment closures: Grad and Bi-Gaussian
- Numerical flux: Rusanov scheme
- Computational grid: medium resolution ($\approx 65{,}000$ cells)
- Comparison against DSMC reference solutions

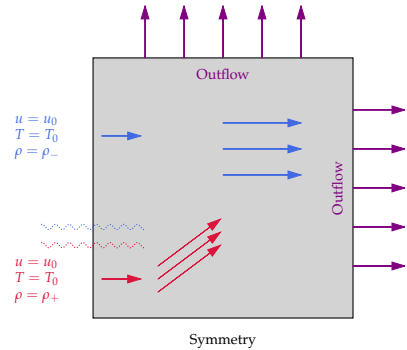

Schematic of the 2D computational configuration

Comparison of density fields

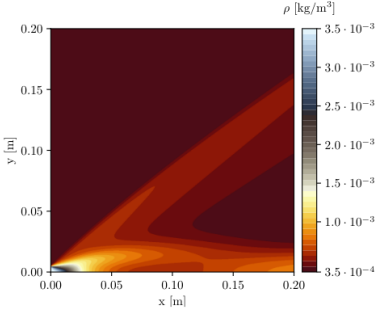

Grad method

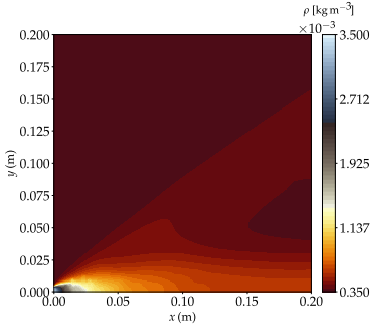

Bi-Gaussian method

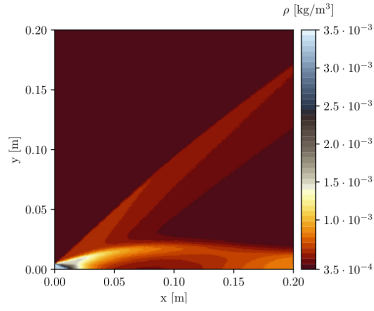

Reference DSMC

Comparison of heat flux fields

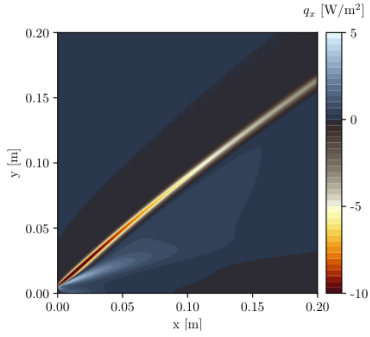

Grad method

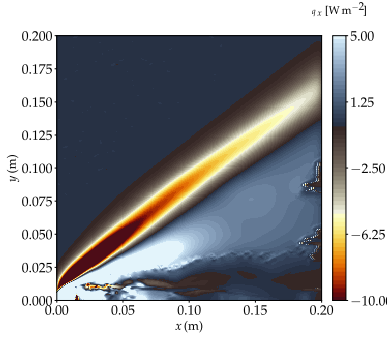

Bi-Gaussian method

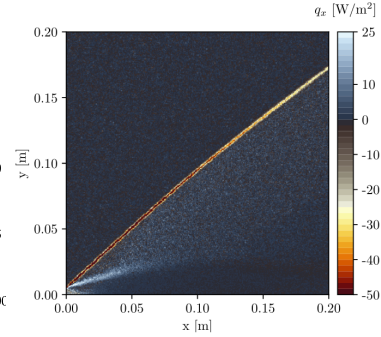

Reference DSMC

RÉPUBLIQUE FRANÇAISE
Liberté
Égalité
Fraternité

ONERA
THE FRENCH AEROSPACE LAB

ÉCOLE POLYTECHNIQUE
IP PARIS

CMAP

SMAI
société de mathématiques appliquées et industrielles

Thank you for listening! Any questions?

References

[1] M. R. A. Abdelmalik et al., "Moment Closure Approximations of the Boltzmann Equation Based on φ-Divergences", Journal of Statistical Physics **164**, 77–104 (2016).

[2] A. Berger et al., "Comparison of high-order moment models for the ion dynamics in a bounded low-temperature plasma", Physics of Plasmas **32**, 103503 (2025).

[3] P. Bernigaud et al., "Simulation of hybrid dense-rarefied flows relying on relaxation schemes and a hierarchy of moment methods", in Advances in entry systems modeling: modeling summer visit 2025 technical reports, NASA/TM-20260002490 (2026), pp. 54–58.

[4] P. L. Bhatnagar et al., "A model for collision processes in gases", Physical Review **94**, 511–525 (1954).

[5] G. Boillat et al., "On the shock structure problem for hyperbolic system of balance laws and convex entropy", Continuum Mechanics and Thermodynamics **10**, 285–292 (1998).

[6] Z. Cai, "Moment method as a numerical solver: challenge from shock structure problems", Journal of Computational Physics **444**, 110593 (2021).

[7] C. Cercignani, *Mathematical Methods in Kinetic Theory*, (Springer US, Boston, MA, 1990).

[8] C. Cercignani et al., *The mathematical theory of dilute gases*, (Springer New York, 1994).

[9] C. Chalons et al., "Multivariate Gaussian Extended Quadrature Method of Moments for Turbulent Disperse Multiphase Flow", Multiscale Modeling & Simulation **15**, 1553–1583 (2017).

[10] C. Chalons et al., "Beyond pressureless gas dynamics: quadrature-based velocity moment models", 10.48550/ARXIV.1011.2974 (2010).

[11] J. H. Ferziger et al., "Mathematical Theory of Transport Processes in Gases", American Journal of Physics **41**, 601–603 (1973).

[12] R. O. Fox et al., "Conditional hyperbolic quadrature method of moments for kinetic equations", Journal of Computational Physics **365**, 269–293 (2018).

References (cont.)

[13] H. Grad, "On the kinetic theory of rarefied gases", Communications on Pure and Applied Mathematics **2**, 331–407 (1949).
[14] C. P. T. Groth, *Moment closures and kinetic equations*, Lecture notes for the course AER1301: Moment Closure Methods for Kinetic Equations of Complex Transport Phenomena, 2020.
[15] Z. Hu et al., "Numerical Simulation of Microflows Using Hermite Spectral Methods", SIAM Journal on Scientific Computing **42**, B105–B134 (2020).
[16] M. Junk, "Domain of definition of levermore's five-moment system", Journal of Statistical Physics **93**, 1143–1167 (1998).
[17] D. Kah, "Taking into account polydispersity for the modeling of liquid fuel injection in internal combustion engines", Theses (Ecole Centrale Paris, Dec. 2010).
[18] F. Laurent et al., "Evaluation of the 1-D hyperbolic quadrature method of moments for non-equilibrium flows", ESAIM: Proceedings and Surveys **76**, 52–67 (2024).
[19] C. D. Levermore, "Moment closure hierarchies for kinetic theories", Journal of Statistical Physics **83**, 1021–1065 (1996).
[20] T. Pichard, "Some recent advances on the method of moments in kinetic theory", ESAIM: Proceedings and Surveys **75**, edited by M. Doumic et al., 86–95 (2023).
[21] M. Pigou et al., "New developments of the extended quadrature method of moments to solve population balance equations", Journal of Computational Physics **365**, 243–268 (2018).
[22] T. Ruggeri, "Breakdown of shock-wave-structure solutions", Physical Review E **47**, 4135–4140 (1993).
[23] T. Schwartzentruber et al., "A hybrid particle-continuum method applied to shock waves", Journal of Computational Physics **215**, 402–416 (2006).
[24] M. Torrilhon, "Hyperbolic Moment Equations in Kinetic Gas Theory Based on Multi-Variate Pearson-IV-Distributions", Communications in Computational Physics **7**, 639–673 (2010).

References (cont.)

[25] M. Torrilhon, "Modeling Nonequilibrium Gas Flow Based on Moment Equations", Annual Review of Fluid Mechanics **48**, 429–458 (2016).

[26] C. Villani, "A review of mathematical topics in collisional kinetic theory", in *Handbook of mathematical fluid dynamics* (Elsevier, 2002), 71–74.

[27] C. Virgile et al., "Optimisation of a hybrid NS–DSMC methodology for continuous–rarefied jet flows", Acta Astronautica **195**, 295–308 (2022).

[28] K. Xu et al., "A unified gas-kinetic scheme for continuum and rarefied flows", Journal of Computational Physics **229**, 7747–7764 (2010).

[29] W. Yang et al., "Comparative study of the discrete velocity and the moment method for rarefied gas flows", in 31st International Symposium on Rarefied Gas Dynamics: RGD31, Vol. 2132 (2019), p. 120006.

Appendix – Moments and Macroscopic variables

1D1V five-moment model:

$$M_k = m\int_{\mathbb{R}} \xi^k f \,\mathrm{d}\xi, \qquad C_k = m\int_{\mathbb{R}} (\xi - u)^k f \,\mathrm{d}\xi.$$

Macroscopic quantities

$\rho = M_0$ (density)

$u = \dfrac{M_1}{M_0}$ (bulk velocity)

$p = C_2$ (pressure)

$q = C_3$ (heat flux)

$r = C_4$ (4th-order moment)

$s = C_5$ (5th-order moment)

State vector:

$$\mathbf{Q} = (\rho, u, p, q, r)^{\mathsf{T}}$$

Appendix – Non dimensionalization

Starting point: BGK-based moment equations for $\langle \xi^k f \rangle$, $k = 0, \dots, 4$

Non-dimensional variables:

$$\bar{t} = \frac{t}{t_0}, \qquad \bar{x} = \frac{x}{\sqrt{\theta_0} t_0}, \qquad \bar{\xi} = \frac{\xi}{\sqrt{\theta_0}}, \qquad \bar{f} = \frac{\sqrt{\theta_0}}{\rho_0 / m} f$$

Dimensionless moment equations:

$$\frac{\partial}{\partial \bar{t}} \langle \bar{\xi}^k \bar{f} \rangle + \frac{\partial}{\partial \bar{x}} \langle \bar{\xi}^{k+1} \bar{f} \rangle = -\frac{1}{\mathrm{Kn}} \langle \bar{\xi}^k (\bar{f} - \bar{\mathcal{M}}) \rangle, \qquad k = 0, \dots, 4$$

Note. For convenience, dimensionless variables will be used, and bars are omitted

Appendix – Five-Moment system

Governing equations (BGK relaxation model)

$$
\begin{aligned}
&\frac{\partial}{\partial t}\rho + \frac{\partial}{\partial x}(\rho u) = 0,\\
&\frac{\partial}{\partial t}(\rho u) + \frac{\partial}{\partial x}\left(\rho u^2 + p\right) = 0,\\
&\frac{\partial}{\partial t}\left(\rho u^2 + p\right) + \frac{\partial}{\partial x}\left(\rho u^3 + 3pu + q\right) = 0,\\
&\frac{\partial}{\partial t}\left(\rho u^3 + 3pu + q\right) + \frac{\partial}{\partial x}\left(\rho u^4 + 6pu^2 + 4qu + r\right) = -\frac{q}{\tau},\\
&\frac{\partial}{\partial t}\left(\rho u^4 + 6pu^2 + 4qu + r\right) + \frac{\partial}{\partial x}\left(\rho u^5 + 10pu^3 + 10qu^2 + 5ru + s\right) = -\frac{1}{\rho}\left(4uq + r - \frac{3p^2}{\rho}\right)
\end{aligned}
$$

The last two equations include collision terms, relaxing q and r toward equilibrium

Appendix – Five-Moment system (cont.)

Compact vector form

$$\frac{\partial \mathbf{M}}{\partial t} + \frac{\partial \mathbf{F}}{\partial x} = \mathbf{S},$$

with

$$\mathbf{M}(\mathbf{Q}) = \begin{pmatrix} \rho \\ \rho u \\ \rho u^2 + p \\ \rho u^3 + 3pu + q \\ \rho u^4 + 6pu^2 + 4qu + r \end{pmatrix}, \qquad \mathbf{F}(\mathbf{Q}) = \begin{pmatrix} \rho u \\ \rho u^2 + p \\ \rho u^3 + 3pu + q \\ \rho u^4 + 6pu^2 + 4qu + r \\ \rho u^5 + 10pu^3 + 10qu^2 + 5ru + s \end{pmatrix},$$

$$\mathbf{S}(\mathbf{Q}) = \begin{pmatrix} 0 \\ 0 \\ 0 \\ -q/\tau \\ -(4uq + r - 3p^2/\rho)/\rho \end{pmatrix}$$

Appendix – Algebraic structure

The flux Jacobian is

$$\mathbf{J} = \frac{\partial \mathbf{F}}{\partial \mathbf{U}} = \begin{pmatrix} 0 & 1 & 0 & \cdots & 0 \\ 0 & 0 & 1 & \cdots & 0 \\ \vdots & \vdots & \vdots & \ddots & \vdots \\ 0 & 0 & 0 & \cdots & 1 \\ a_0 & a_1 & a_2 & \cdots & a_{N-1} \end{pmatrix},$$

with $a_k = \frac{\partial \hat{M}_N}{\partial M_k}$

Its characteristic polynomial is

$$\chi_{\mathbf{J}}(\lambda) = \lambda^N - \sum_{k=0}^{N-1} a_k \lambda^k$$

Closure requirement: The system is *strongly hyperbolic* if eigenvalues of $\mathbf{J}$ are real and distinct

Appendix – Sub-shock formation

Shock-structure solutions

- A shock structure is a smooth travelling-wave profile connecting two equilibrium states
- Its existence relies on dissipative mechanisms to regularize the hyperbolic dynamics

Boillat–Ruggeri theorem (Boillat et al., (1998); Ruggeri, (1993))

Let u^- be an upstream equilibrium state and s the shock velocity. If

$$s > \lambda_{\max}(u^-),$$

no C^1 shock structure can exist between equilibrium states
Any admissible shock profile must therefore contain at least one sub-shock

Mechanism of sub-shock formation

- The shock-structure ODE becomes singular when

$$s = \lambda_i(U)$$

along the profile
- Physically: the shock propagates faster than all information carriers upstream
- Dissipation is insufficient to enforce a smooth transition $\Rightarrow$ internal discontinuity

Appendix – Sub-shock formation (cont.)

Sub-shocks in monatomic gases (Rational Extended Thermodynamics)

- For the Grad 13-moment system, the condition

$$s > \lambda_{\max}(u^-)$$

corresponds to a critical Mach number

$$\mathrm{Ma} \gtrsim 1.65,$$

above which sub-shocks are unavoidable

Appendix – Time integration via operator splitting

Separate transport and collisions in the BGK-based moment system

$$\frac{\partial \mathbf{M}}{\partial t} + \nabla_x \cdot \mathbf{F}(\mathbf{M}) = \mathbf{S}(\mathbf{M}), \qquad \mathbf{S} = \frac{1}{\tau}\left(\mathbf{M}^{\mathrm{eq}} - \mathbf{M}\right)$$

Splitting strategy (over Δt):

i. **Transport step:** solve the homogeneous system

$$\frac{\partial \mathbf{M}}{\partial t} + \nabla_x \cdot \mathbf{F}(\mathbf{M}) = 0$$

to obtain an intermediate state $\mathbf{M}^*$ (using a finite-volume scheme)

ii. **Collision step:** solve the local ODE

$$\frac{\partial \mathbf{M}}{\partial t} = \frac{1}{\tau}\left(\mathbf{M}^{\mathrm{eq}} - \mathbf{M}\right)$$

at each grid point

First-order splitting:

$$\mathbf{M}_i^* = \mathbf{M}_i^n - \frac{\Delta t}{\Delta x}\left(\mathbf{F}_{i+1/2}^n - \mathbf{F}_{i-1/2}^n\right), \qquad \mathbf{M}_i^{n+1} = \mathbf{M}_i^* + \Delta t\, \mathbf{S}(\mathbf{M}_i^*)$$

Appendix – Exact integration of BGK collision

- During the collision substep, $\mathbf{M}^{\mathrm{eq}}$ is constant
- The ODE admits the exact solution

$$\mathbf{M}(t+\Delta t) = \mathbf{M}^{\mathrm{eq}} + \big(\mathbf{M}(t) - \mathbf{M}^{\mathrm{eq}}\big)e^{-\Delta t/\tau}$$

- Collision update in splitting:

$$\mathbf{M}_i^{n+1} = \mathbf{M}_i^{\mathrm{eq}} + \big(\mathbf{M}_i^{*} - \mathbf{M}_i^{\mathrm{eq}}\big)e^{-\Delta t/\tau}$$

Advantages: unconditionally stable, no stiffness constraints when $\tau \ll \Delta t$

Appendix – Grad's classical closure

Idea: approximate the distribution function using a truncated polynomial expansion around a Maxwellian Grad, (1949)

$$\hat{f}(v) = \frac{\mathcal{M}(\rho, u, \theta)}{\rho} \sum_{\alpha=0}^{N} f_\alpha \, \theta^{-\alpha/2} \mathrm{He}_\alpha \left(\frac{v-u}{\sqrt{\theta}} \right)$$

Main characteristics

- Exact near Maxwellian equilibrium
- Coefficients computed explicitly via orthogonality
- Reduced computational cost and straightforward extension to multi-D

Drawbacks

- Not positivity-preserving
- Not globally hyperbolic

} Accurate only for weakly non-equilibrium flows (numerical instabilities far from equilibrium, Levermore, (1996))

Appendix – Linearized Grad closure

Idea: linearize the Hermite expansion around fixed parameters $(\overline{u}, \overline{\theta})$ Hu et al., (2020)

$$\hat{f}(v) = \frac{1}{\sqrt{2\pi\overline{\theta}}} \sum_{\alpha=0}^{N-1} f_\alpha \hat{\theta}^{-\alpha/2} \mathrm{He}_\alpha\left(\frac{v-\overline{u}}{\sqrt{\overline{\theta}}}\right) e^{-\frac{(v-\overline{u})^2}{2\overline{\theta}}}$$

Main characteristics

- Equivalent to a Hermite spectral method
- Globally hyperbolic (constant characteristic speeds)

Drawbacks

- Accuracy highly sensitive to parameter selection (Cai, (2021))
- Parameters must be selected manually

Appendix – Quadrature-based closures

Idea: reconstruct the distribution function as a weighted sum of kernels κ

$$\hat{f}(v) = \sum_{\alpha=1}^{N} \varrho_\alpha \, \kappa_\sigma(v - \zeta_\alpha)$$

Main characteristics

- Realizability guaranteed by construction
- Quadrature parameters $(\varrho_\alpha, \zeta_\alpha)$ obtained via moment inversion

Drawbacks

- Nonlinear and potentially ill-conditioned inversion procedure
- Extension to higher-dimensional velocity spaces is non-trivial
- Lack of global hyperbolicity and associated entropy inequality
- No general guarantee of uniqueness for weak solutions (Chalons et al., (2010); Kah, (2010))

Appendix – Hyperbolic QMOM (HyQMOM) closure

Idea: construct the closure using central moments and orthogonal polynomials, with *Dirac delta kernels* representing the quadrature nodes Fox et al., (2018)

- Quadrature nodes chosen via Chebyshev algorithm
- Closure derived directly from moment relations (no explicit VDF reconstruction)

Main characteristics

- Realizability guaranteed by construction
- Global hyperbolicity

Drawbacks

- Difficult extension to multidimensional spaces
- Discrete representation of the distribution function

Appendix – Multi-Gaussian closure

Idea: replace Dirac deltas with *Gaussian* kernels Chalons et al., (2017); Pigou et al., (2018)

$$\hat{f}(v) = \sum_{\alpha=1}^{N} \frac{\varrho_\alpha}{\sigma\sqrt{2\pi}} \exp\left(-\frac{(v-\zeta_\alpha)^2}{2\sigma^2}\right)$$

Bi-Gaussian closure ($N = 2$)

- Five-moment system
- Smooth, continuous distribution

Main characteristics

- Global hyperbolicity

Drawback

- Defined only on a subset of the realizability domain (mapping moment vector $\leftrightarrow$ kernel parameters not globally invertible, Berger et al., (2025))

Appendix – Entropy-based closures

Idea: reconstruct $\hat{f}$ by minimising an entropy functional under moment constraints

$$\hat{f} = \arg\min_{f \geq 0} \left\{ \int_{\mathbb{R}} \eta(f)\, \mathrm{d}v \right\}, \qquad \int_{\mathbb{R}} v^k f \, \mathrm{d}v = M_k$$

Maximum Entropy Levermore, (1996)

Generator: $\eta = f \log f - f$

$$\hat{f}(v) = \exp\left(\sum_{k=0}^{n-1} \lambda_k \, v^k \right)$$

φ-Divergence Abdelmalik et al., (2016)

Deformed exponential, order q:

$$\hat{f}(v) = \mathcal{M}(\bar{u}, \bar{\theta}) \left(1 + \frac{\sum_{k=0}^{n-1} \lambda_k \, v^k}{q} \right)_+^q$$

Main characteristics

- Global hyperbolicity and thermodynamic consistency
- φ-div $\rightarrow$ No Junk-line: well-posed for all realizable moments

Drawback

- High cost: nonlinear optimisation per cell
- MaxEnt$\rightarrow$ Junk-line pathology Junk, (1998): undefined on subset of realizability domain
- φ-div $\rightarrow$ Background $\mathcal{M}$ must be chosen carefully

Appendix – Iterative inversion strategies

Bi-Gaussian, MaxEnt, and φ-divergence require solving a *nonlinear system* at every cell and time step to recover the closure parameters from the retained moments

Bi-Gaussian

Ansatz: sum of two Gaussians

$$\hat{f} = \sum_{i=1}^{2} \frac{w_i}{\sqrt{2\pi\theta_i}} e^{-\frac{(v-u_i)^2}{2\theta_i}}$$

Parameters (w_i, u_i, θ_i) found by matching moments $(M_0, \dots, M_4)$

Strategy: iterations on the nonlinear moment-matching system

Maximum Entropy

Ansatz: exponential family

$$\hat{f} = \exp\left(\sum_{k=0}^{n-1} \lambda_k v^k\right)$$

Multipliers (λ_k) found by solving the dual optimisation problem

$$\min_{\lambda} \int_{\mathbb{R}} \eta^*(\boldsymbol{\lambda}^\top \boldsymbol{v})\, \mathrm{d}v - \boldsymbol{\lambda}^\top \mathbf{M}$$

Strategy: Newton–Raphson on the gradient of the dual functional; sensitive to initialisation

φ-divergence

Ansatz: deformed exponential

$$\hat{f} = \mathcal{M}(\overline{u}, \overline{\theta}) \left(1 + \frac{\sum_{k=0}^{n-1} \lambda_k v^k}{q}\right)_+^q$$

Truncated power approximation of the exponential — regularises the tail behaviour

Strategy: Newton iterations on the same dual structure as MaxEnt; Maxwellian shape parameter $\overline{u}$, $\overbrace{\theta}$ must be chosen carefully